Altered brain functional networks in Internet gaming disorder: Independent component and graph theoretical analysis under a probability-discounting task

Ziliang Wang [a], Xiaoyue Liu [b,a], Yanbo Hu [c], Hui Zheng [a], Xiaoxia Du [d], Guangheng Dong [a, e*]

[a] Department of Psychology, Zhejiang Normal University, Jinhua, P.R. China.

[b] School of Mental Health, Wenzhou Medical University, Wenzhou, Zhejiang, China

[c] Department of Psychology, London Metropolitan University, London, U.K.

[d] Department of Physics, Shanghai Key Laboratory of Magnetic Resonance, East China Normal University, Shanghai. P.R. China.

[e] Institute of Psychological and Brain Sciences, Zhejiang Normal University, Jinhua, P.R. China.

*** Corresponding author:**

Guangheng Dong, Ph.D., Professor.

Department of Psychology, Zhejiang Normal University, 688 Yingbin Road, Jinhua, Zhejiang Province, P.R. China. 321004.

E-mail: dongguangheng@zjnu.edu.cn

Abstract

Objectives: Internet gaming disorder (IGD) is becoming a matter of concern around the world. However, the neural mechanism underlying IGD remains unclear. The paper is to explore the differences between the neuronal network of IGD participants and that of recreational game users (RGU) participants.

Methods: Imaging and behavioral data were collected from 18 IGD and 20 RGU participants under a probability-discounting task. The independent component analysis (ICA) and graph theoretical analysis (GTA) were used to analysis the data.

Results: Behavioral results showed the IGD participants, compared to RGU, prefer risky options to the fixed ones and spent less time in making risky decisions. In imaging results, the ICA analysis revealed that the IGD showed stronger functional connectivity (FC) in reward circuits and executive control network, as well as lower FC in anterior salience network (ASN) than RGU; for the GTA results, the IGD showed impaired FC in reward circuits and ASN compared to RGU.

Conclusions: These results suggest that IGD participants were more sensitive to rewards and they were more impulsive in decision-making as they could not control their impulsivity effectively. This might explain why IGD participants cannot stop their gaming behaviors even when facing severe negative consequences.

Keywords: ICA; GTA; possibility-discount task; executive control; reward circuits

1. Introduction

As a typical non-substance related addiction, Internet gaming disorder (IGD) is defined as people unable to control their desires to play Internet games excessively. Studies have revealed that IGD can lead to severe negative consequences, such as impaired physical and psychological states, social deficits, and/or poor academic performance [1,2]. In 2013, the DSM-5 committee included the IGD in the section III of the DSM-5 as an issue warranting further study [3-5], and a diagnostic criteria for IGD was proposed, which facilitated potential studies [6].

Most people like games, however, only a few of them are addicted to them, most of the players play games in a recreational way [7]. They can play games in a controlled manner without showing psychiatric symptoms of addiction, such as craving, conflict and withdrawal [8-10]. These people are defined as recreational Internet gaming users (RGU) [11].

Similar to gambling addiction [12], the fifth edition of the Diagnostic and Statistical Manual of Mental Disorders (DSM-5) introduced Internet gaming disorder in the research appendix; at the same time, the International Classification of Diseases (ICD-11) is also considering it as a behavioral addiction [13].The IGD participants shared similarities with traditional addictions including higher impulsivity, unsuccessful cognitive control, deficit in decision-making [14-16], higher sensitivity to rewards [17], and neglect their losses in daily-life situations [10,18]. Studies have also found that IGD participants are more likely to make decisions with greater risk tendencies than healthy controls [16,19]. Comparing to RGU, the IGD participants showed decreased frontal brain responses during processing of losing outcomes, suggesting their

decreased loss sensitivity during making-decision [11]. These findings were consistent with the results using substance use disorders or pathological gambling participants [20-22].

Rational decision-making describes one's ability to make the best choice from multiple alternatives, which is important in exploring ones choice features in risky situations. Probability discounting (PD) tasks measures the tradeoffs between reward magnitudes and probabilities to examine the decision-making features under risky situations. Participants need to make a choice between a large amount of money with a low probability of winning and a small amount of money with a high and fixed probability of winning. Choosing the larger amount of money with lower probability of winning showed a higher subjective value for probabilistic rewards, which reflects the tendency to take risks. Although most people would choose the fixed one to avoid getting nothing , the IGD participants preferred to choose the larger amount of money with lower probability of winning [19,23]. As this feature of PD, in this study, we would use PD task to explore the neuronal network underlying decision-making process of IGD participants.

Previous IGD studies mostly focused on the specific functions of a brain region, but how these brain regions interact together is still lacking in understanding. In this study, we combined two analyses (independent component analysis (ICA) and graph theoretical analysis (GTA) to explore the differences between the neuronal network of IGD participants and that of RGU participants using a probability-discounting task.

Independent component analysis (ICA) is a data-driven technique that can extract the information about the intrinsic neuronal functional connectivity without cognitive tasks [24].

Previously we found that IGD showed impaired executive control network compared with the healthy control [19] and they also exhibited enhanced sensitivity to reward and an impaired executive control ability when performing a delayed discounting task [25]. Graph theoretical analysis (GTA) regards the whole brain as a complex network, composed of a set of nodes and edges [26]. It quantitatively measures each node by incorporating connectivity information from the complete network, reflecting the integrated nature of local brain activity. Previous studies have demonstrated that human brain anatomical and functional networks have small-world properties [27,28] i.e. high level of clustering coefficient and short path length linking all nodes [29]. Recently, a study has found that there are significant differences in regional nodal characteristics of IGD comparing to that of healthy participants during resting-state [30]. The ICA focuses on a specific group of brain areas, while the GTA measures the nodes and edges of the whole brain. These two approaches are complementary in that they look at different aspects of the brain network [31].

The second strength we have in this study is the subject selection. Most previous studies focused on the differences between the IGD and healthy controls (HC), which have some limitations. The IGD participants played online games frequently, however, the HC group are none or low-frequent game players, they have limited experience with online gaming. Hence, we selected the RGU as comparison group to overcome these limitations. Thus, the current study used RGU as control group to find some features of IGD in a PD task.

In our previous studies and other studies, we found the IGD participants group show impaired decision-making in probability-discounting task.. They were also more impulsive in decision-making and could not effectively control their impulsivity [10,11,16,32]. Based on these

results, in this PD task, we hypothesized that the IGD participants would chose lower probability discounting when making decisions, which may be related to the impairment of reward circuits and executive control ability. We combined the ICA and GTA methods to explore dysfunctional networks in IGD to gain a better understanding about the neural mechanism of IGD and to provide insights for better treatment strategies for people with IGD.

2. Methods

2.1 participants

This experiment conformed to The Code of Ethics of the World Medical Association (Declaration of Helsinki) and was approved by the Human Investigations Committee of Zhejiang Normal University. All participants provided written informed consent before the formal scan session.

Forty right-handed male university students (20 IGD, 20 RGU) were recruited in this study. Only males were included because of the high IGD prevalence in males. There was no significant age difference between the two groups (Table 1). All participants underwent structured psychiatric interviews (MINI) conducted by an experienced psychiatrist [33]. The MINI results revealed that all participants were free from psychiatric/neurological disorders. No participants reported previous gambling or illicit drugs (e.g., marijuana, heroin) experiences. All participants were instructed not to use any medicine or substances including coffee, tea, and alcohol, on the day of scanning.

IGD participants were selected based on a Young's Internet Addiction Test (IAT) and the nine DSM-5 criteria of IGD [1,34]. Participants were diagnosed with IGD if they satisfied the

following three criteria: (1) scored 50 or higher on the IAT scores; (2) reached at least five DSM-5 criteria; (3) spent at least 80% of online time playing games and spent at least 2 hours per day in online games during the last 2 years.

For RGU participants, firstly, most of them scored less than 50 on the IAT, less than five DSM-V criteria and were not affecting their daily life. Secondly, RGU should be a minimum of 2 years and without showing any symptoms of physical or psychological dependence. Thirdly, the RGU participants played online games more than 14 hours per week and a minimum 5 of 7 days in a week [17]. The two groups showed significant differences in IAT and DSM scores (Table 1).

	IGD (n = 18)	RGU(n = 20)	*t*	*p*
Age	21.61 ± 2.40	21.84 ± 2.43	0.29	0.773
IAT Score	66.72 ± 10.06	41.45 ± 9.04	8.16	0.000
DSM-5 Score	5.89 ± 0.83	2.65 ± 0.99	10.86	0.000
Game Playing, Hours/Week	20.22 ± 7.09	19.85 ± 5.62	0.18	0.858

Table1. Demographic information and group differences.

2.2 Task and procedure

During the experiment, participants firstly completed an informed consent form and the Matters of Attention of functional magnetic resonance imaging (fMRI). Secondly, they were provided with a sample PD task. To motivate participants making their choices seriously, we told them that they would be paid after the experiment according to their choice in a randomly selected trial of the task. If they chose the certain option, he would receive the money in cash. If they selected the probabilistic option, he could select a card from many cards of two colors (red and black) reflecting the probability of receiving the money. Finally, they completed the PD task in the fMRI scanner. During the task, participants were told to make choices between a fixed but small amount of money and a probabilistic but larger amount of money available based on a probability value (i.e. 10 Yuan 100% versus 14 Yuan 40%) (Figure 1).

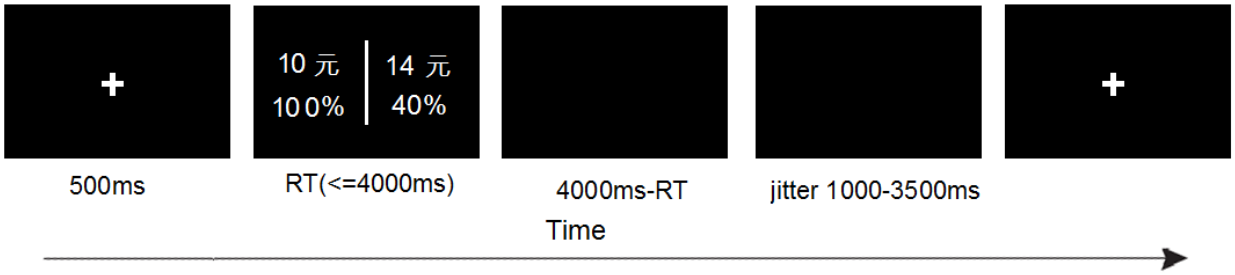

Figure 1.

The probabilistic choices ranged from 10% to 20%, 30%, 40%, 50%, 60%, 70%, 80%, 90%, and monetary amounts ranged from 11 to 12.5,14, 17, 20, 25, 33, 50 and 100 Yuan. There were 81 trials in total and took approximately 15 minutes. Stimuli were randomly presented and behavioral data was collected using the E-prime software (Psychology Software Tools, Inc.).

2.3 Behavioral data analysis

Two participants were excluded from data analysis because of large head movements and/or choosing the same options in all trials. As a result, the remaining data of 38 participants (18 IGD, 20 RGU) were included in data analysis. PD task contains a large but probabilistic reward against a small but fixed reward. In PD task, discounting means the devaluation of an outcome when the outcome is obtained probabilistically. PD rates were calculated by using a hyperbolic function [23,35], which represented as follows:

$$V = \frac{A}{(1+hO)}, \quad O = (\frac{1}{P} - 1) \qquad (1)$$

The V represents the discounted value, and the A is monetary reward. P represents the probability to receive rewards, and O represents the odds against receiving the rewards. The h value is a subject specific discounting constant. Notably, smaller values of h might suggest a tendency to take risks and more impulsivity. It can represent cognitive impulsivity features affecting decision-making process. One important procedure for calculating h is to determine indifferent points, which are points that the subjective value of a probabilistic option is equivalent to that of the other fixed option. The analysis procedure was composed of two steps: Firstly, a non-linear curve-fitting program was applied to data in Origin 7.0 to calculate each subject's best-fit-h value from Eq [36]. Secondly, a log 10 transformation of the h values was performed. By this transformation, the distribution of values was normal [37].

2.4 Image acquisition and pre-processing

All participants underwent the fMRI scan in a Siemens Trio 3-Tesla scanner (Siemens, Magnetom Trio Tim). The sequence parameters were as follows: repetition time (TR)=2000ms; echo time (TE)=30ms; flip angle 90°; interleaved sequence; 33 slice per volume; 3 mm

thickness; field of view 220 *220 mm^2; and matrix 64 *64. All stimuli were presented by the Invivo synchronous system (Invivo Company, www.invivocorp.com/) through a monitor in the head coil. Structural images covering the whole brain were collected through a T1-weighted three-dimensional spoiled gradient-recalled sequence (176 slices, flip angle = 15°, echo time = 3.93 ms, slice thickness = 1.0 mm, skip = 0 mm, inversion time 1100 ms, field of view = 240 × 240 mm, in-plane resolution = 256 × 256).

Imaging analysis was performed using SPM8 (http://www.fil.ion.ucl.ac.uk/spm). Images were slice-timed, reoriented, and realigned to the first volume. Then, T1-co-registered volumes were normalized to an SPM EPI template and spatially smoothed by using an 8 mm FWHM Gaussian kernel. No participant was eliminated due to large head motion coefficients based on the criteria (head motion <2 mm and 2 degrees).

2.5 Independent component analysis

The group ICA was applied to the preprocessed fMRI data within a toolbox (GIFT v2.0) implemented in Matlab R2012a (http://icatb.sourceforge.net). The fMRI data was reduced through two principal component analysis (PCA) stages [38,39]. The default component number was 20 and a spatial ICA was conducted to estimate the 20 mutually independent components using Fast ICA algorithm, which is a stochastic process [24]. ICASSO algorithm [40] was performed to remedy the problem, which repeated the ICA analysis multiple times and then output a final set of independent components, providing a measurement of consistency between different ICA runs. Eventually, a single ICA time course and an independent functional spatial map for every subject were obtained.

2.5.1 Component selection

There are two steps for selecting components of interest. Each ICA component spatial map was correlated with probabilistic maps of gray matter (GM), cerebral spinal fluid (CSF) and white matter (WM) within a standardized brain space provided by the MNI templates in SPM5. Firstly, components showing relatively high correlations with WM and CSF and low correlation with GM were considered as artifacts and should be discarded. Components that satisfied the threshold of $r^2 < 0.025$ for CSF and WM and $r^2 > 0.05$ for GM were reserved and considered as meaningful. Thus, this analysis would exclude noise related components that represented eye movement, head motion, ventricular pulsations, and other signal artifacts [41]. The second step was to select the components that were highly correlated with the experimental tasks from the remaining components based on the first analysis. A multiple temporal regression was performed on the ICA time courses with the GLM design matrix to estimate the association between the experimental task and the independent components, which resulted in a set of beta weights for each subject and each condition (probability and certain). Then, an independent one-sample t-test ($p < 0.05$) on beta weights for the IGD and RGU groups were examined under each task condition. The beta weight of components that differed significantly from zero indicated a significant association with the experimental tasks, whereas components failed to show a significant relationship were diagnosed as task-irrelevant and discarded.

2.5.2 Between-group comparison of components

Components that passed the two criterions were subjected to between-group task-related activity comparison analysis. An independent two sample t-test ($p< 0.05$) on the beta weights of each remaining component between the RGU and IGD groups was performed in the GIFT toolbox.

2.5.3 Correlations between behavioral performances and brain activities

We analyzed the correlation between behavioral performances and the beta weights for IGD and RGU participants separately. Specifically, we analyzed correlations among beta weights, reaction time (RT), and probability discounting rate (the *h* values). Further, the correlation between beta weights and the addiction severity (the IAT and DSM scores) were also examined.

2.6 Graph theoretical analysis

2.6.1 Components and voxels selection

For this method, ICA was used to detect the strongest PD task-related components. One sample t-tests of beta values for each component were performed to define task-related components [42]. According to the above results and the features of the task, we selected three components to perform the remaining analysis. In the study, we used 95 voxels to assess their small-world properties for three brain networks separately. All voxels in each component were sorted from high to low according to their *Z*-scores and the top 95 voxels (most task-related) constituted the three task-related networks.

2.6.2 Estimation of the partial correlations

We used partial correlation to measure connectivity between a given pair of voxels, and built undirected graphs respectively for three networks. The partial correlation matrix is a symmetric matrix, filtering out the contributions of all other variables; each off-diagonal element is the correlation coefficient between a pair of variables. The first stage was to estimate the sample covariance matrix S from the data matrix Y= (x_i), i=1,…, 95, for each individual. Here x_i was the time series of each *i*th voxel. If we introduce X= (x_j x_k) to represent the observations in

the *j*th and *k*th voxels, Z=Y\X represent the other 93 time series matrices. Each component of S contains the sample covariance value between two voxels (say *j* and *k*). If the covariance matrix of [X, Z] was

$$S = \begin{pmatrix} S_{11} & S_{12} \\ S_{12}^{T} & S_{22} \end{pmatrix}, \quad (2)$$

In which S_{11} was the covariance matrix of X, S_{12} was the covariance matrix of X and Z and S_{22} was the covariance matrix of Z, then the partial correlation matrix of X, controlling for Z could be defined formally as a normalized version of the covariance matrix, $S_{xy} = S_{11} - S_{12} S_{22}^{-1} S_{12}^{T}$. Finally, a Fisher's r-to-z transformation [43] was used on the partial correlation matrix to induce normality on the partial correlation coefficients.

2.6.3 Constructing brain network

An $N \times N$ ($N = 120$ in the present study) binary graph brain network, *G*, consisting of nodes (brain voxels) and undirected edges (connectivity) between nodes, could be constructed by applying a predefined threshold *T* to the partial correlation coefficients:

$$e_{ij} = \begin{cases} 1 & if \ |z(i,j)| \geq T \\ 0 & otherwise \end{cases} \quad (3)$$

If the absolute value of correlation between *i* and *j* was larger than the predefined threshold *T*, an edge was said to exist; otherwise it did not exist. The selection of threshold T will be discussed in following sections.

2.6.4 Small-worldness

The small-world properties including clustering coefficient (C_{net}), normalized clustering coefficient (γ), characteristic path length (L_{net}), normalized characteristic path length (λ), global

efficiency (E_{global}), local efficiency (E_{local}), and small-worldness (δ). Small-world networks have lower path lengths but higher clustering coefficients, that is $\gamma=C_{net}/C_{random} > 1$, $\lambda=L_{net}/L_{random}=1$ [44,45]. Combined these two conditions, we can get a scalar quantitative measurement of small-world networks, small-worldness, $\delta=\gamma/\lambda$, which is typically > 1 [46]. We applied a wide range sparsity threshold T to all correlation matrices. The range of T was determined according to the following criteria: 1) the average degree of all nodes of each network was larger than 2×log (N) [47]. N is the number of nodes (here, N=120); 2) the small-worldness scalars of each threshold network was larger than 1.0 for all participants. This criteria guaranteed the threshold networks had as few spurious edges in sparse properties as possible [28]. Thus, the range of our generated sparsity threshold of C9 was 0.07<T<0.4 with an interval of 0.01. The range of our generated sparsity threshold of C10 was 0.10<T<0.28 with an interval of 0.01 (one RGU subject was excluded because most δ were smaller than 1.0). The range of our generated sparsity threshold of C20 was 0.23<T<0.4 with an interval of 0.01(one RGU subject was excluded because most δ were smaller than 1.0). Next, we calculated global network metrics at each sparsity threshold. Moreover, the area under the curve (AUC) that independent of single threshold was calculated for global network metrics in order to provide a summarized scalar for the topological organization of brain networks [28].

2.6.5 Statistical analysis

To determine the differences between the IGD and RGU groups in small-world properties, a two-sample two-tailed *t*-test with a threshold of $p<0.05$ was performed on the AUC of each metric for three task related networks (C_{net}, L_{net}, E_{global}, E_{local}, γ, λ, and σ) separately. Also, we performed the two-sample *t*-test on each metric of three networks at each sparsity threshold level.

2.6.6 Relationships between Network Metrics and Behavioral Scores

We calculated the correlations between small-world properties that group-level differences of each network and behavioral data and IAT and DSM scores.

3. Results

3.1 Behavioral performance

The independent sample *t*-test on the logged *h* values indicated that the IGD group showed lower log (*h*) values than the RGU group, $t = 2.22$, $p = 0.03$. The mean *h* values for IGD and RGU were 1.94; 4.21 (Figure 2a), suggesting a more rapid rate of PD for IGD than the RGU group (Figure 2b). The R^2 value for probability discounting functions (0.84 for IGD and 0.81 for RGU) represented the accounted variance by Eq. (1). Finally, the data of RT (RT probability - RT certain) were subjected to an independent sample t-test, and the result showed that the RT (RT probability - RT certain) of IGD is much shorter compared with that of RGU (IGD = 47±132ms, RGU：129±255ms, t =1.22, p=0.23. Correlation analysis between the log (*h*) values and the RT showed that they were positively correlated (r=0.529, p<0.001) (Figure 2c).

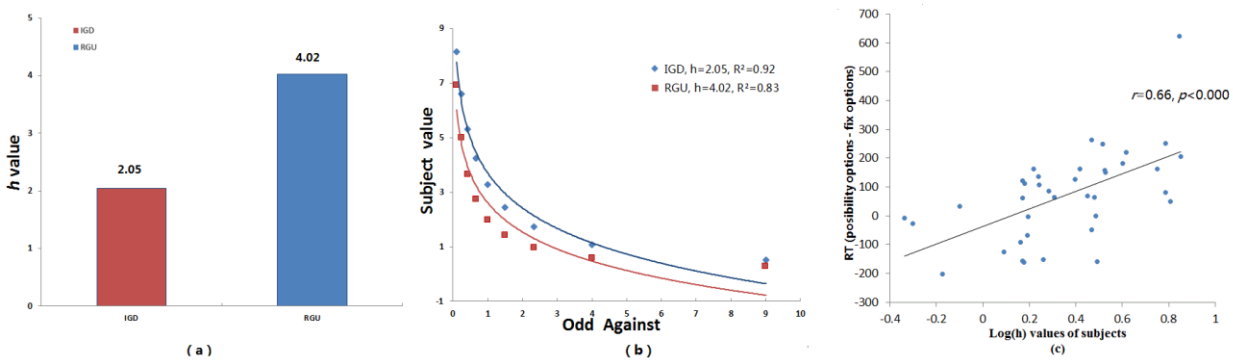

Figure2

3.2 ICA results

3.2.1 Independent component

Six out of twenty components (C4, C9, C10, C11, C15, and C20) passed our selection criteria.

Component	Mean±SD		*t*-value (RGU-IGD)	*p*
	RGU subjects (n = 20)	IGD subjects (n = 18)		

These six components had a relatively low spatial correlation with cerebral spinal fluid and white while a high correlation with grey. Also, these components showed significant correlation with the experimental task.

3.2.2 Between-group differences

A two-sample *t* test was used to determine whether the beta weights that were produced by a regression showed statistically significant difference under probability or certain conditions. C9, C10 and C20 showed significant difference under the two conditions (Table 2).

C9				
Probability	0.44±2.16	1.78±1.87	-2.14	0.04
Certain	-0.74±1.94	1.02±1.84	-3.02	0.00
C10				
Probability	-1.76±2.52	-3.49±3.23	1.93	0.06
Certain	-0.90±2.51	-2.90±3.07	2.32	0.03
C20				
Probability	-0.64±3.94	2.32±3.56	-2.56	0.01
Certain	-0.86±3.65	2.03±3.28	-2.71	0.01

Table 2: Components that showed significant differences in two-sample t-tests of beta weights.

Under the probability condition, C9 was positively modulated by the condition and the IGD group showed higher task-related activity than RGU. Under the probability and certain conditions, C10 was negatively modulated by the two conditions and the IGD group showed marginally lower task-related activity than RGU. For C20, the IGD and RGU group were modulated in different directions under the two conditions. C20 was positively modulated in IGD group and negatively modulated in RGU group under the probability and certain conditions. To identify which networks the three components belong to, we contrasted each component of these brain regions with the fourteen brain networks [48]. Consequently, component 9 was involved in left executive control network (ECN), which mainly consists of the prefrontal and parietal cortices. Component 10 was involved in anterior salience network (ASN), primarily including anterior insula, dorsal anterior cingulate cortex. Component 20 was involved in Basal Ganglia Network (BGN), primarily including the striatum and the thalamus (Figure 3).

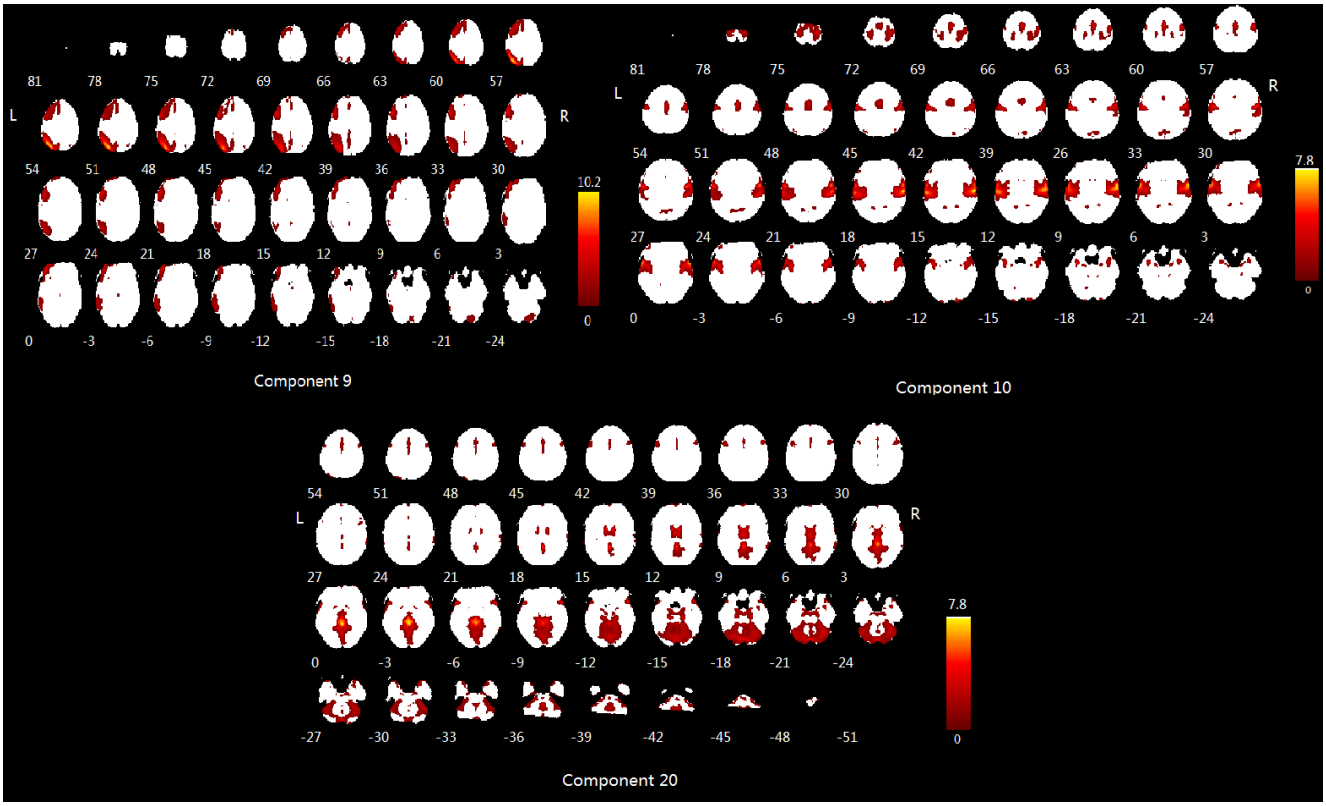

Figure 3.

3.2.3 Correlation analysis results

We analyzed the correlation between task behavioral performances and the beta weights of C9, C10 and C20. There was a significant positive correlation between the beta values (beta $_{probability}$ – beta $_{certain)}$ of C10 and the logged *h* values only in RGU participants (r= 0.481, p= 0.032) (Figure 4).

Figure

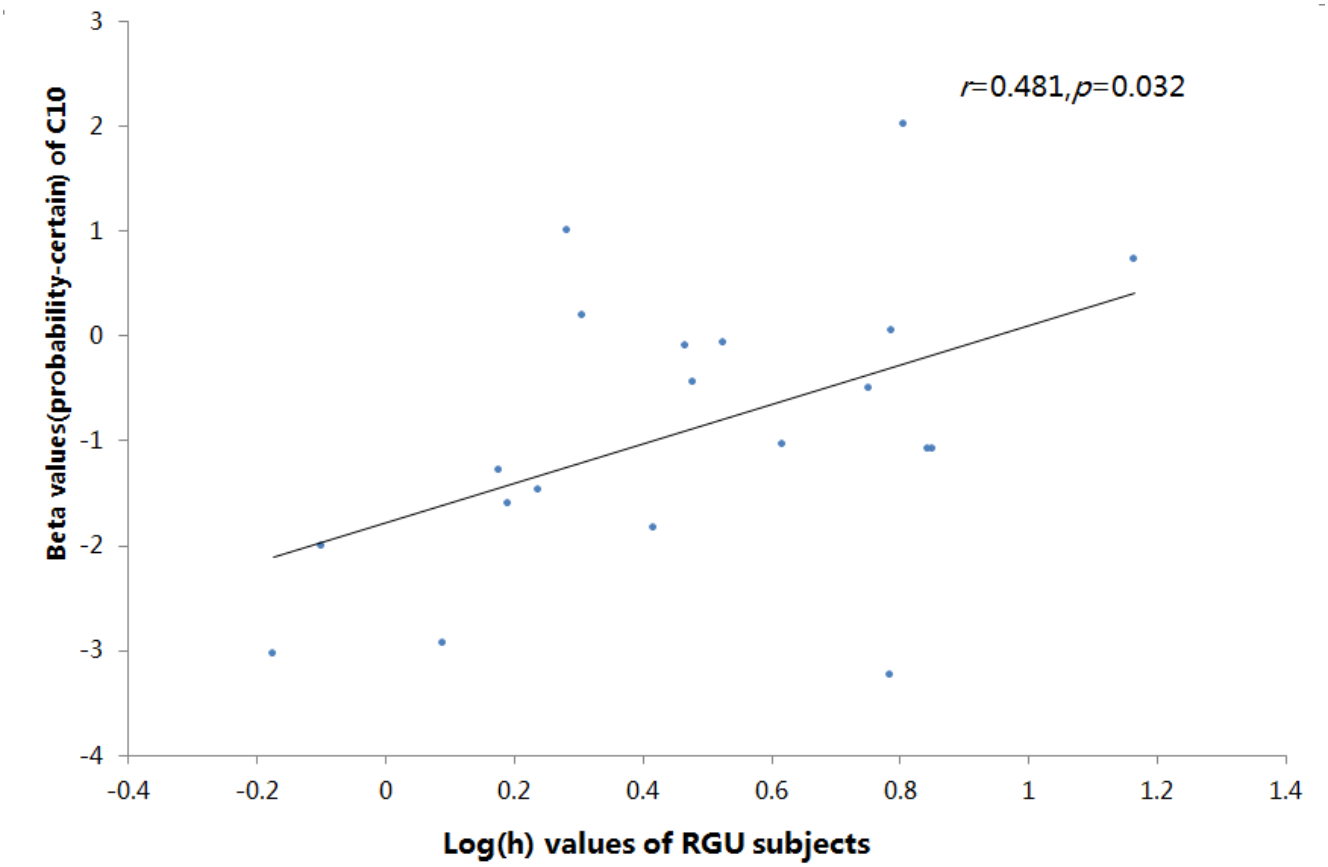

Figure 4.

3.3 Graph theoretical analysis results

3.3.1 Small-world properties

The results showed that the three functional networks of all participants had similar characteristic path lengths ($\lambda \approx 1$) but higher clustering coefficients ($\gamma > 1$), and the small-worldness, $\delta = \gamma/\lambda$ (> 1). Hence, the IGD group and RGU all showed typical features of small-world topology in these networks. Despite common small-world architecture, the results revealed that significant differences in small-world attributions between IGD participants and RGU participants. A two-sample *t* test on AUC values showed group differences in these three networks. For the BGN, the IGD showed significant higher clustering coefficient than RGU on AUC values (t=2.388, p=0.022). Although other properties did not reach the significant, the trends are in existence. The IGD showed higher λ (t=1.749, p=0.088) and lower E_{global} (t=

-1.742, p=0.089) than RGU participants. For the anterior salience network, the IGD showed lower clustering coefficient (t= -1.807, p=0.079) and higher E_{global} (t=1.755, p=0.088) than RGU (Table 3).

Table 3 Small-world properties that showed significant differences in two-sample t-tests of AUC values.

Small-world properties	Mean±SD		*t*-value (IGD-RGU)	*p*
	RGU subjects	IGD subjects		
C10				
C_{net}	0.23±0.058	0.23±0.058	-1.807	0.079
E_{global}	0.17±0.008	0.18±0.006	1.755	0.088
C20				
C_{net}	0.22±0.059	0.23±0.065	2.388	0.022
λ	0.41±0.107	0.42±0.017	1.749	0.088
E_{global}	0.18±0.005	0.176±0.007	-1.742	0.089

For each threshold level, the IGD showed significantly lower clustering coefficient and higher $E_{global,}$ and shorter path length in the anterior salience network (Figure 5a). In the BGN, the IGD showed significantly higher cluster coefficient and higher E_{local} (Figure 5b) and lower E_{global} and longer path length and longer normalized path length in each 18 threshold levels (Figure 5c). In the ECN with 34 threshold levels, the IGD group showed lower E_{global} and longer path length than RGU group (not significant).

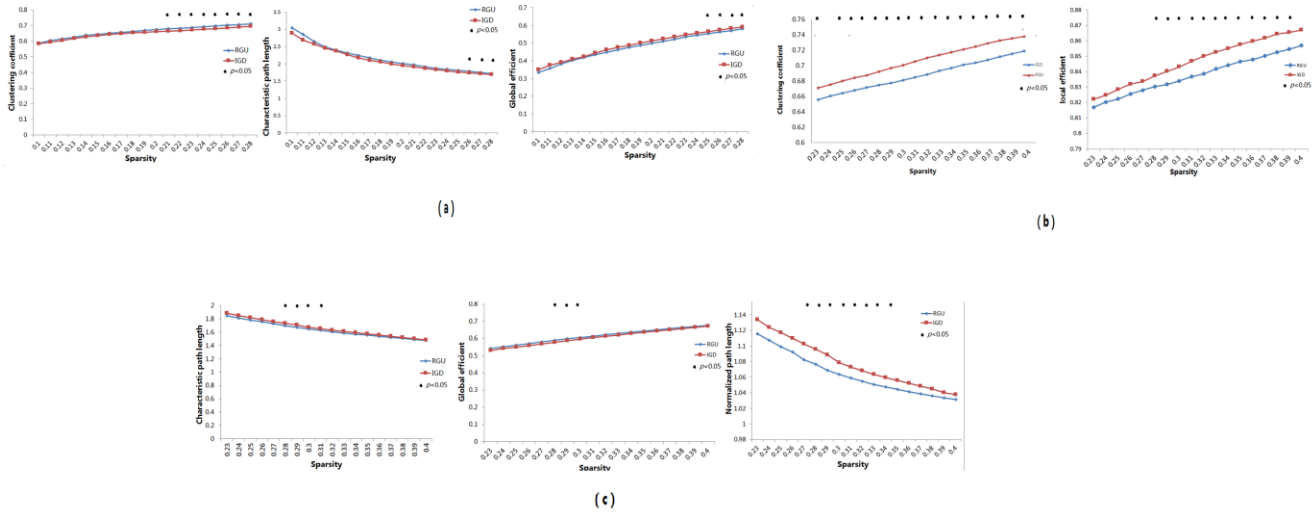

Figure5

3.3.2 Correlation between Network metrics and Behavioral measures

We explored the relationships of network metrics with both behavioral and addiction severity (the DSM and IAT scores) of all participants. Correlation analysis demonstrated that the observed global abnormalities were correlated with the IAT scores and behaviors. Significant positive correlations (p<0.05) were found between IAT scores and AUC values of clustering coefficient in the BGN (r=0.324, p=0.047) (Figure 6a). The AUC value of E_{global} was negatively correlated with the logged h values in the ASN (r=-0.319, p=0.054) (Figure 6b). In the executive control network, the AUC values of normalized cluster coefficient negatively correlated with the RT (r=-0.284, p=0.085) (Figure 6c). Although some of these correlations did not reach the statistical significance, the trends are in existence.

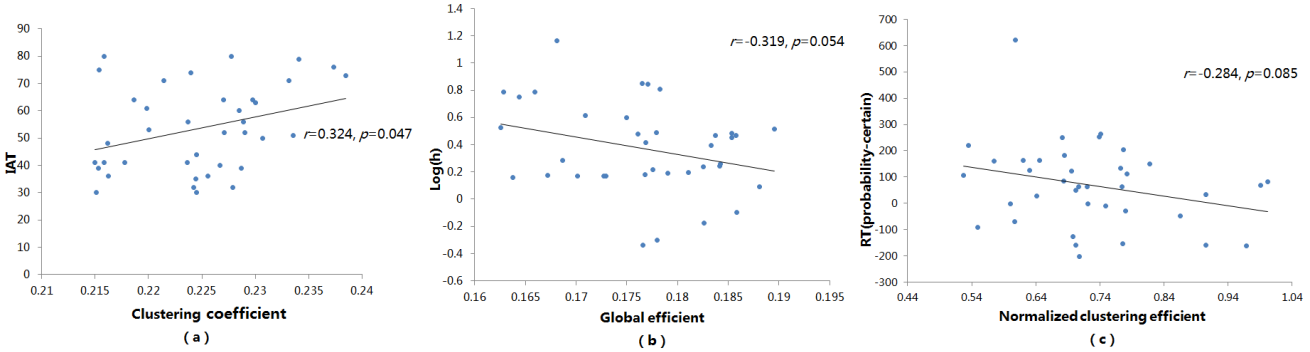

4. Discussion

The current study explored the potential changed neuronal networks of IGD participants using ICA and GTA. The behavior results showed that the IGD group were associated with lower probability discounting of risky options and spent less time during decision-making compared to RGU. The lower *h* values might suggest a tendency to take risks and increased level of impulsivity [49-51]. This suggested that the IGD group was poor in risk evaluation and impulse control compared to RGU. Positive correlation between PD rate and RT indicated that the ones who were higher impulsivity with more quickly in making decisions without extra thinking. In imaging results, the ICA and GTA results both showed dysfunction networks connectivity in ASN and BGN.

4.1 Executive control network (ECN)

The ECN was involved in cognitive control and goal-directed behaviors [52]. Previous studies have revealed that brain training games could improve executive functions for individuals [53,54]. However, it was not the same for excessive Internet games. A study using the ReHo method found that IGD showed higher nervous activity of ECN compared with HCs [55,56]. Our previous study found that the IGD group exhibited stronger FC in ECN when selecting small but immediate options [25]. In this study, the ICA results showed that the IGD participants enhanced FC of ECN compared to RGU in probability and certain conditions, which may suggest that the ECN engaged more in IGD participants than RGU in making decisions. Even so, the IGD participants still failed to control their risky behaviors and preferred lower probability and higher risky choices. In behavioral performance, the IGD group showed lower probability

discounting than RGU, which suggests that the IGD group is more impulsive than RGU [49,50]. Numerous studies had detected the possible neural mechanisms of the IGD and suggested that it may be related to the impaired cognitive control [25,57]. Hence, we speculated that the IGD participants impaired the ability to inhibit their impulse and to make better choice under a risky circumstance.

4.2 Anterior salience network (ASN)

The ASN plays an important role in identifying relevant internal and external stimuli in order to guide and modulate cognitive behaviors [58]. One theory is that the salience network, which includes the anterior cingulate cortex and insula regulates dynamic changes in other brain core networks to modulate cognitive behaviors [59,60].

For ICA results, the IGD participants showed lower beta weights in ASN under the PD task, which suggested that the IGD participants decreased FC of ASN compared to RGU. A traumatic brain injury study has found the disruption of this network could lead to inefficient cognitive control [60,61]. Additionally, reduced structural and effective connectivity within the salience network have been found to be related with impaired individuals' cognitive control function [59,61]. We found that the beta weights of ASN were positively correlated with the log(h) values, which suggested that the higher risk the weaker FC of the ASN. It was consistent with our ICA results. These results suggested that the IGD used less time to consider the different condition and could not efficiently control impulsivity and guide their behaviors.

For small-world results, significant group differences were observed in the clustering coefficient, characteristic path length and E_{global} showed at each threshold level. IGD had lower

values in clustering coefficient, lower characteristic path length, and higher E_{global} values than RGU. A small amount of long-range connections are not only good for connection separation of local nerve and connection cost constraint, but also for long distance information transmission and integration for brain regions [62]. A study has showed when the E_{global} of MCI patients has increased, their ability to process long-distance information ability has also improved [63]. In our study, the small-world results showed that the inner brain regions' connections have difference in IGD, with lower clustering coefficient than RGU participants. This may reveal that the ability of IGD participants to process local information is impaired. The IGD showed shorter path length and higher E_{global}, which suggested that the ability to process local information was decreased, under the compensatory mechanism, the ability to process the long distance information would have been improved. The E_{global} had negative correlation with the probability discounting of the ASN. In addition, the lower logged *h* values, the higher global efficient also suggested that the ASN of IGD was impaired: they cannot effectively identify the external risks, and failed to guide their behavior in a more rational way when making decisions. Combining these two results, we concluded that the disturbed connectivity within anterior salience network may be related to the failure of risky behavior regulation and this inefficient regulation was contributed in the impaired cognitive control in IGD participants.

4.3 Basal ganglia network (BGN)

Neuroimaging studies suggested that the BGN plays a critical role in mediating the subjective reward effects [64,65]. Reward circuits mainly involve in evaluating the values of both stimuli and rewards before making a decision [66].

For ICA results, the IGD showed stronger FC in the BGN than the RGU, and this phenomenon was congruent with previous studies [67,68]. The different levels of FC of BGN might be explained by the different sensitivities to the rewards [69,70]. A review reported significant hyperactivity in BGN of gambling disorder [71]. Some studies have suggested that the reward circuits have been changed in IGD participants [72-74]. The IGD showed more sensitivity towards reward, and reduced sensitivity of punishment [18,25,75]. A study has shown that the IGD are associated with enhanced FC of BGN, which suggests IGD participants have enhanced sensitivity to rewards when making decisions [25]. In comparison with RGU, the participants with IGD showed shorter RT when choosing the risky options, which might suggest that the IGD participants with made their decisions hastily irrespective of the potential loss.

For small-world results, the IGD group showed higher clustering coefficient, higher E_{local}, longer path length and lower E_{global} compared to the RGU group at each threshold level. It has been suggested that lower clustering coefficient and lower E_{local} mean relatively sparse local connectivity; a short path length and high E_{global} represent the high synchronization of brain functional networks [76]. Higher clustering coefficient reflects disrupted neuron integration between distant regions, which has relatively sparse long-distant and relatively dense short-distant functional connections in the internet addiction disorder group [77]. In this study, the clustering coefficient of the reward network has positively correlation with IAT scores, the higher IAT scores the higher the clustering coefficient. This reflects disrupted neuronal integration between distant regions with the severity of addiction. The addictive behaviors may lead to the disconnection of long distance connections and may encourage the establishment of short distance connections within clusters as an alternative path to keep information transmission between two distant regions. However, establishment of short distance

connections may introduce abnormal clusters, which increases the risk of creating an uncontrolled information flow through the entire network. The IGD groups were more likely to choose the lower probability discounting and spend less time making decisions in PD task. The IGD participants preferred the large monetary rewards with low probability to the certain small monetary rewards. Taken together, the dysfunction network connectivity in IGD might suggest that the IGD groups are more sensitivity to reward and neglect the potential risky when making choices.

5. Conclusions

The present study examined the functional organization of the brain networks for the IGD participants under a PD task using ICA and GTA. The results revealed connectivity of three brain networks (ASN, ECN and BGN) were altered in IGD compared to RGU participants. Taking the role of these networks into consideration, the current study suggests that Internet game addicts are more impulsive in decision-making and cannot effectively control their impulsivity because of their impaired executive control ability. The changes in these networks were involved in decision-making and cognitive control and may be a key mechanism preventing recreational game players from the risk of developing addiction.

Limitations

Several limitations should be mentioned for this study. Firstly, non-gamer group that have no experience of gaming can be collected to look at different between the three groups (healthy control, IGD and RGU). The results will be more interesting including the non-gamer group. And only male college students were recruited for this study. It will be necessary for further researches to include female participants and to explore gender effect in IGD. Secondly, the

IAT is not a specific test for IGD and we did not measure the impulsivity by BIS-11 or the UPPS. The lack of behavioral support for many of the results only provides a possible explanation that needs to be further explored later. In future research, we should collect more behavioral data, which could provide more supports to imaging results. Thirdly, undirected, unweighted networks are built in the present study [78]. A weighted network could provide more information in the future studies [79]. Besides, the data smoothing during preprocessing. Spatial smoothing could result in artificial correlations between voxels by previous voxel-based network analysis studies [80]. Partial correlation will remove local correlations (including the correlation caused by smoothing) but preserve the unique voxel variance. Further researches are needed to determine the full effect of smoothing on correlations and partial correlations, including their relationship to variability between participants.

Acknowledgements

Ziliang Wang and Xiaoyue Liu contributed equally. Ziliang Wang and Xiaoyue Liu analyzed the data and wrote the first draft of the manuscript. Hui Zheng contributed to experimental programming and data preprocessing. Xiaoxia Du contributed to fMRI data collection. Guangheng Dong & Yanbo Hu designed the research, revised and improved the manuscript. All authors contributed to and had approved the final manuscript.

Competing interests

The authors declared that there were no competing interests exist.

Role of the funding source

This research was supported by National Science Foundation of China (31371023). The

funders had no further role in study design; in the data collection, analyses and interpretation; the decision to publish, or preparation of the manuscript.

Data accessibility

Data are available upon request from the corresponding author at dongguangheng@zjnu.edu.cn.

References

1. Petry NM, Rehbein F, Gentile DA, et al. An international consensus for assessing internet gaming disorder using the new DSM-5 approach. *Addiction.* 2014;109(9):1399.
2. Meng Y, Deng W, Wang H, Guo W, Li T. The prefrontal dysfunction in individuals with Internet gaming disorder: a meta-analysis of functional magnetic resonance imaging studies. *Addiction Biology.* 2014;20(4):799.
3. Király O, Nagygyörgy K, Griths MD, Demetrovics Z. *Problematic Online Gaming.* 2014.
4. Julie M, Frédéric M, Magali N, et al. Massively multiplayer online role-playing games: comparing characteristics of addict vs non-addict online recruited gamers in a French adult population. *BMC Psychiatry.* 2011;11(1):144.
5. Gentile DA, Choo H, Liau A, et al. Pathological video game use among youths: a two-year longitudinal study. *Pediatrics.* 2011;127(2):e319.
6. AmericanPsychiatricAssociation. *Diagnostic and statistical manual of mental disorders.* American Psychiatric Pub, Washington DC; 2013.
7. Montag C, Reuter M. *Internet Addiction: Neuroscientific Approaches and Therapeutical Interventions.* Springer Publishing Company, Incorporated; 2015.
8. Viriyavejakul C. Recreational Gaming Behavior of Undergraduate Students in Thailand. 2008.
9. Kuss DJ, Griffiths MD. Internet Gaming Addiction: A Systematic Review of Empirical Research. *International Journal of Mental Health and Addiction.* 2012;10(2):278-296.
10. Wang Y, Wu L, Wang L, Zhang Y, Du X, Dong G. Impaired decision‐making and impulse control in Internet gaming addicts: evidence from the comparison with recreational Internet game users. *Addiction Biology.* 2016.
11. Dong G, Li H, Wang L, Potenza MN. Cognitive control and reward/loss processing in Internet gaming disorder: Results from a comparison with recreational Internet game-users. *European Psychiatry.* 2017;44:30-38.
12. Bae S, Hong JS, Kim SM, Han DH. Bupropion Shows Different Effects on Brain Functional Connectivity in Patients With Internet-Based Gambling Disorder and Internet Gaming Disorder. *Frontiers in Psychiatry.* 2018;9.
13. Petry NM, Zajac K, Ginley MK. Behavioral Addictions as Mental Disorders: To Be or Not To Be? *Annual Review of Clinical Psychology.* 2016;14(1):399-423.
14. Ko CH, Hsieh TJ, Wang PW, et al. Altered gray matter density and disrupted functional connectivity of the amygdala in adults with Internet gaming disorder. *Progress in neuro-psychopharmacology & biological psychiatry.* 2015;57:185.
15. Dong G, Potenza MN. A cognitive-behavioral model of Internet gaming disorder: theoretical underpinnings and clinical implications. *Journal of Psychiatric Research.* 2014;58(8):7–11.

16. Dong G, Potenza MN. Risk-taking and risky decision-making in Internet gaming disorder: Implications regarding online gaming in the setting of negative consequences. *Journal of Psychiatric Research.* 2016;73(1):1.
17. Dong G, Wang L, Du X, Potenza MN. Gaming Increases Craving to Gaming-Related Stimuli in Individuals Wth Internet Gaming Disorder. *Biological Psychiatry Cognitive Neuroscience & Neuroimaging.* 2017.
18. Dong G, Hu Y, Xiao L. Reward/punishment sensitivities among internet addicts: Implications for their addictive behaviors. *Progress in neuro-psychopharmacology & biological psychiatry.* 2013;46(5):139-145.
19. Wang L, Wu L, Lin X, et al. Dysfunctional default mode network and executive control network in people with Internet gaming disorder: Independent component analysis under a probability discounting task. *European Psychiatry.* 2016;34:36.
20. Gilman JM, Calderon V, Curran MT, Evins AE. Young adult cannabis users report greater propensity for risk-taking only in non-monetary domains. *Drug & Alcohol Dependence.* 2015;147:26-31.
21. Schutter DJLG, Bokhoven IV, Vanderschuren LJMJ, Lochman JE, Matthys W. Risky Decision Making in Substance Dependent Adolescents with a Disruptive Behavior Disorder. *Journal of Abnormal Child Psychology.* 2011;39(3):333.
22. Madden GJ, Petry NM, Johnson PS. Pathological gamblers discount probabilistic rewards less steeply than matched controls. *Experimental & Clinical Psychopharmacology.* 2009;17(5):283-290.
23. Madden GJ, Petry NM, Johnson PS. Pathological gamblers discount probabilistic rewards less steeply than matched controls. *Experimental & Clinical Psychopharmacology.* 2009;17(5):283-290.
24. Calhoun VD, Adali T, Pearlson GD, Pekar JJ. A method for making group inferences from functional MRI data using independent component analysis. *Human Brain Mapping.* 2001;14(3):140.
25. Wang Y, Wu L, Zhou H, et al. Impaired executive control and reward circuit in Internet gaming addicts under a delay discounting task: independent component analysis. *European Archives of Psychiatry & Clinical Neuroscience.* 2016:1-11.
26. He Y, Evans A. Graph theoretical modeling of brain connectivity. *Current Opinion in Neurology.* 2010;23(4):341-350.
27. Newman MEJ. Newman MEJ.. The structure and function of complex networks. SIAM Rev 45: 167-256. 2003;45(2):167-256.
28. Achard S, Bullmore E. *Efficiency and Cost of Economical Brain Functional Networks.* PLoS Comput Biol; 2007.
29. Kim DI, Manoach DS, Mathalon DH, et al. Dysregulation of working memory and default-mode networks in schizophrenia using independent component analysis, an fBIRN and MCIC study. *Human Brain Mapping.* 2009;30(11):3795-3811.
30. Wang L, Wu L, Lin X, et al. Altered brain functional networks in people with Internet gaming disorder: Evidence from resting-state fMRI. *Psychiatry Research Neuroimaging.* 2016;254:156.
31. Ye Z, Doã±Amayor N, Mã¼Nte TF. Brain network of semantic integration in sentence reading: insights from independent component analysis and graph theoretical analysis. *Human Brain Mapping.* 2014;35(2):367-376.
32. Dong G, Hu Y, Lin X. Reward/punishment sensitivities among internet addicts: Implications for their addictive behaviors. *Progress in neuro-psychopharmacology & biological psychiatry.* 2013;46(5):139.

33. Lecrubier Y, Sheehan DV, Weiller E, et al. The Mini International Neuropsychiatric Interview (MINI). A short diagnostic structured interview: reliability and validity according to the CIDI. *European Psychiatry.* 1997;12(5):224–231.
34. Young K. Internet Addiction: Diagnosis and Treatment Considerations. *Journal of Contemporary Psychotherapy.* 2009;39(4):241-246.
35. Yi R, Chase WD, Bickel WK. Probability discounting among cigarette smokers and nonsmokers: molecular analysis discerns group differences. *Behavioural Pharmacology.* 2007;18(7):633-639.
36. Rachlin H, Raineri A, Cross D. Subjective probability and delay. *Journal of the Experimental Analysis of Behavior.* 1991;55(2):233-244.
37. Young KS. Internet Addiction: The Emergence of a New Clinical Disorder. *Cyberpsychology & Behavior.* 1998;1(3):237-244.
38. Mitchell SH. Measures of impulsivity in cigarette smokers and non-smokers. *Psychopharmacology.* 1999;146(4):455-464.
39. Reynolds B, Richards JB, Horn K, Karraker K. Delay discounting and probability discounting as related to cigarette smoking status in adults. *Behavioural Processes.* 2004;65(1):35-42.
40. Bell AJ, Sejnowski TJ. An information-maximization approach to blind separation and blind deconvolution. *Neural Computation.* 1995;7(6):1129-1159.
41. Himberg J, Hyvärinen A, Esposito F. Validating the independent components of neuroimaging time series via clustering and visualization. *Neuroimage.* 2004;22(3):1214.
42. Meda SA, Stevens MC, Folley BS, Calhoun VD, Pearlson GD. Evidence for anomalous network connectivity during working memory encoding in schizophrenia: an ICA based analysis. *Plos One.* 2009;4(11):e7911.
43. Salvador R, Suckling J, Coleman MR, Pickard JD, Menon D, Bullmore E. Neurophysiological architecture of functional magnetic resonance images of human brain. *Cerebral Cortex.* 2005;15(9):1332-1342.
44. Fisher R. On the 'Probable Error' of a Coefficient of Correlation Deduced From a Small Sample. *Metron.* 1920;1.
45. Liu Y, Liang M, Zhou Y, et al. Disrupted small-world networks in schizophrenia. *Brain.* 2008;131(4):945-961.
46. Watts DJ, Strogatz SH. Collective dynamics of 'small-world' networks. *Nature.* 1998;393(6684):440-442.
47. Zhang J, Wang J, Wu Q, et al. Disrupted brain connectivity networks in drug-naive, first-episode major depressive disorder. *Biological Psychiatry.* 2011;70(4):334-342.
48. Widyanto L, Griffiths MD, Brunsden V. A psychometric comparison of the Internet Addiction Test, the Internet-Related Problem Scale, and self-diagnosis. *Cyberpsychology Behavior & Social Networking.* 2011;14(3):141-149.
49. Dai Z, Harrow SE, Song X, Rucklidge JJ, Grace RC. Gambling, Delay, and Probability Discounting in Adults With and Without ADHD. *Journal of Attention Disorders.* 2013;20(11):968.
50. Reynolds B, Richards JB, Horn K, Karraker K. Delay discounting and probability discounting as related to cigarette smoking status in adults. *Behav Processes.* 2004;65(1):35-42.
51. Holt DD, Green L, Myerson J. Is discounting impulsive?. Evidence from temporal and probability discounting in gambling and non-gambling college students. *Behavioural Processes.* 2003;64(3):355-367.
52. Shirer W, Ryali S, Rykhlevskaia E, Menon V, Greicius M. Decoding subject-driven cognitive states with whole-brain connectivity patterns. *Cerebral Cortex.* 2012;22(1):158-165.
53. Krmpotich TD, Tregellas JR, Thompson LL, Banich MT, Klenk AM, Tanabe JL. Resting-state

activity in the left executive control network is associated with behavioral approach and is increased in substance dependence. *Drug & Alcohol Dependence.* 2013;129(1-2):1.
54. Sutherland MT, Mchugh MJ, Pariyadath V, Stein EA. Resting state functional connectivity in addiction: Lessons learned and a road ahead. *Neuroimage.* 2012;62(4):2281-2295.
55. Rui N, Taki Y, Takeuchi H, et al. Brain Training Game Boosts Executive Functions, Working Memory and Processing Speed in the Young Adults: A Randomized Controlled Trial. *Plos One.* 2013;8(2):-.
56. Rui N, Yasuyuki T, Hikaru T, et al. Brain Training Game Improves Executive Functions and Processing Speed in the Elderly: A Randomized Controlled Trial. *Plos One.* 2012;7(1):e29676.
57. Dong G, Lin X, Hu Y, Xie C, Du X. Imbalanced functional link between executive control network and reward network explain the online-game seeking behaviors in Internet gaming disorder. *Sci Rep-Uk.* 2015;5(1):97.
58. Bonnelle V, Ham TE, Leech R, et al. Salience network integrity predicts default mode network function after traumatic brain injury. *Proceedings of the National Academy of Sciences.* 2012;109(12):4690.
59. Sridharan D, Levitin DJ, Menon V. A Critical Role for the Right Fronto-Insular Cortex in Switching between Central-Executive and Default-Mode Networks. *Proceedings of the National Academy of Sciences.* 2008;105(34):12569.
60. Uddin LQ, Supekar KS, Ryali S, Menon V. Dynamic reconfiguration of structural and functional connectivity across core neurocognitive brain networks with development. *Journal of Neuroscience the Official Journal of the Society for Neuroscience.* 2011;31(50):18578-18589.
61. Menon V. Large-scale brain networks and psychopathology: a unifying triple network model. *Trends in Cognitive Sciences.* 2011;15(10):483-506.
62. Delbeuck X, Linden MVD, Collette F. Alzheimer' Disease as a Disconnection Syndrome? *Neuropsychology Review.* 2003;13(2):79-92.
63. Wang XB, Zhao XH, Jiang H, et al. The Brain Functional Network Efficiency in Patients with Mild Cognitive Impairment. *Chinese Computed Medical Imaging.* 2015.
64. Power Y, Goodyear B, Crockford D. Neural Correlates of Pathological Gamblers Preference for Immediate Rewards During the Iowa Gambling Task: An fMRI Study. *J Gambl Stud.* 2012;28(4):623-636.
65. Dong G, Huang J, Du X. Enhanced reward sensitivity and decreased loss sensitivity in Internet addicts: an fMRI study during a guessing task. *Journal of Psychiatric Research.* 2011;45(11):1525.
66. Zhao Q, Tang Y, Feng H, Li C, Sui D. The effects of neuron heterogeneity and connection mechanism in cortical networks. *Physica A Statistical Mechanics & Its Applications.* 2008;387(23):5952-5957.
67. Yuan K, Wei Q, Yu D, et al. Core brain networks interactions and cognitive control in internet gaming disorder individuals in late adolescence/early adulthood. *Brain Structure and Function.* 2016;221(3):1427-1442.
68. Xing L, Yuan K, Bi Y, et al. Reduced fiber integrity and cognitive control in adolescents with internet gaming disorder. *Brain Research.* 2014;1586(无):109.
69. Moussa MN, Steen MR, Laurienti PJ, Hayasaka S. Consistency of Network Modules in Resting-State fMRI Connectome Data. *Plos One.* 2012;7(8):1036-1036.
70. Schmidt A, Denier N, Magon S, et al. Increased functional connectivity in the resting-state basal ganglia network after acute heroin substitution. *Translational Psychiatry.* 2014;5(3):e533.
71. Meng YJ, Deng W, Wang HY, et al. Reward pathway dysfunction in gambling disorder: A meta-analysis of functional magnetic resonance imaging studies. *Behavioural brain research.*

2014;275:243.
72. Volkow ND, Wang GJ, Fowler JS, Tomasi D, Telang F, Baler R. Addiction: Decreased reward sensitivity and increased expectation sensitivity conspire to overwhelm the brain's control circuit. *Bioessays News & Reviews in Molecular Cellular & Developmental Biology.* 2010;32(9):748-755.
73. Dong G, Huang J, Du X. Enhanced reward sensitivity and decreased loss sensitivity in Internet addicts: An fMRI study during a guessing task. *Journal of Psychiatric Research.* 2011;45(11):1525-1529.
74. Dong G, Wang Y, Potenza MN. The activation of the caudate is associated with correct recollections in a reward‐based recollection task. 2016;37(11):3999-4005.
75. Lorenz RC, Gleich T, Gallinat J, Kühn S. Video game training and the reward system. *Frontiers in Human Neuroscience.* 2015;9:40.
76. Kaiser M, Hilgetag CC. Modelling the development of cortical systems networks. *Neurocomputing.* 2004;s 58–60(3):297-302.
77. Wee CY, Zhao Z, Yap PT, et al. Disrupted Brain Functional Network in Internet Addiction Disorder: A Resting-State Functional Magnetic Resonance Imaging Study. *Plos One.* 2014;9(9):e107306.
78. Lynall ME, Bassett DS, Kerwin R, et al. Functional connectivity and brain networks in schizophrenia. *Journal of Neuroscience.* 2010;30(28):9477-9487.
79. Van Den Heuvel MP, Hulshoff Pol HE. Exploring the brain network: A review on resting-state fMRI functional connectivity. *European Neuropsychopharmacology.* 2010;20(8):519-534.
80. Hayasaka S, Laurienti PJ. Comparison of characteristics between region-and voxel-based network analyses in resting-state fMRI data. *Neuroimage.* 2010;50(2):499.

Figure Legends:

Figure 1: The timeline of one trial in the PD task in the present study.

The fixed (e.g. 10 Yuan 100 percent) options were presented on the left of the screen and the probabilistic (e.g. 14 Yuan 40 percent) options were presented on the right of the screen. In the examples, '元' is the monetary unit of currency in China.

Figure 2: Probability discounting value differences between the IGD and RGU participants. (a) The IGD participants showed the lower *h* value than the RGU group.

(b) Probability discounting functions for IGD and RGU. Points show medial indifferent points for monetary rewards as a function of the odds against receiving the rewards.

(c): Correlation between the log (*h)* value and reaction time in possible minus fixed option.

IGD: Internet gaming disorder; RGU: recreational Internet gaming users. The log (*h)* represents the

probability discounting rate.

Figure 3: Brain areas showing differences in IGD participants compared with RGU group ((IGD possible-IGD fixed)-(RGU possible-RGU fixed)).

Figure 4: Correlation between the log (*h)* value and beta values (probability-certain) of C10. The log (*h)* represents the probability discounting rate. C: component.

Figure 5: (a) The small-world properties of anterior salience network over a range of sparsity threshold. a (1) The IGD participants showed lower clustering coefficient than RGU participants; a (2) The IGD participants showed shorter characteristic path length than RGU participants; a (3) The IGD participants showed higher global efficient than RGU participants. Black dots above indicate significant group difference (p<0.05).

(b) The small-world properties of reward network over a range of sparsity threshold. b (1)The IGD participants showed higher clustering coefficient than RGU participants; b(2) The IGD participants showed higher local efficient than RGU participants. Black dots above indicate significant group difference (p<0.05).

(c) The small-world properties of reward network over a range of sparsity threshold. c (1) The IGD participants showed longer characteristic path length than RGU participants; c (2) The IGD participants showed lower global efficient than RGU participants; c (3) The IGD participants showed longer normalized path length than RGU participants. Black dots above indicate significant group difference (p<0.05).

Figure 6: Correlation between small-world properties and behavior and IAT scores of three brain networks across all participants.

(a) The significant positive correlations (p<0.05) were found between IAT scores and the AUC values of cluster coefficient in reward network.

(b) The AUC values of E_{global} was negatively correlated with the log (*h)* values in the anterior salience network (p<0.05).

(c) The AUC values of normalized cluster coefficient negatively correlated with the RT (p<0.05). AUC: the area under the curve; the log (*h)* represent the discounting rate; RT: reaction time. $E_{global:}$ global efficient.

Table 1: values are presented as mean ± SD. IAT, Internet addiction test; IGD, Internet gaming disorder; RGU, recreational Internet gaming users.

Table 2: Probability means the probability larger option in the PD task, certain means the certain smaller option in the PD task; RGU: recreational Internet gaming users; IGD: Internet gaming disorder; C: component.

Components that showed significant difference between IGD group and RGU group in beta weights (p < 0.05). The beta weights of C10 under both two conditions showed marginally significant difference across the two groups, and the beta weights of C9、C20 were modulated in different directions under the certain condition across the two groups.

Table 3: For the C20, the IGD showed significant higher clustering coefficient than RGU on AUC values (t=2.388, p=0.022). AUC: the area under the curve; RGU: recreational Internet gaming users; IGD: Internet gaming disorder; C: component; C_{net}: clustering coefficient; E_{global}: global efficient; λ: normalized path length.